scientific reports

Check for updates

OPEN

An in vitro accuracy study on scan body-assisted surface based registration for conventional and zygomatic dental implants

Michael D. Han[1]✉, Sebastian Graca[2], Dima Ghunaim[3] & Leila Ahmadian[3]

There are various techniques to measure accuracy of dental implant surgery, but limited data validating the techniques used to analyze accuracy. Scan-body-assisted surface-based registration (SB-SBR) is deemed theoretically accurate, but with challenges in testing accuracy. The purpose of the study was to analyze the accuracy of SB-SBR for conventional (CVI) and zygomatic implants (ZI) using 2 complementary techniques. An in-vitro study was designed using a 3D-printed model of an edentulous maxilla with CVI and ZI digitally planned and placed. SB-SBR was performed on the physical model and on a model-free virtual setting, and the implant position was compared with those of the planned implants 10 times. Outcome variables were angular and linear errors (AE and LE), with thresholds of 1° and 1 mm. Paired t-test and Wilcoxson signed-ranked test were used. Results showed greater AE for ZI versus CVI (mean difference, MD 0.42°). Apical LE was greater for ZI (MD 0.68 mm), while CVI exhibited greater platform LE (MD 0.69 mm). Overall AE remained under 1°, but the apical LE of ZI exceeded 1 mm, which could potentially lead to violation of critical structures when combined with surgical error, highlighting the need for caution when interpreting data derived from SB-SBR especially for ZI.

Quantifying surgical accuracy is essential for improving quality of care, as accuracy data provide the foundation for refining existing surgical techniques and establishing new protocols[1]. In implant dentistry, the importance of analyzing surgical accuracy parallels the continued growth of the field and the development of new techniques, which require accuracy validation to become established as viable treatment modalities.

Many of such new techniques are designed to avoid hard tissue site augmentation, or towards attaining anchorage from remote sites[2,3]. Because of this nature, the risk of surgical complications can be greater in such techniques. Nonaxial implants can obviate the need for alveolar ridge or maxillary sinus augmentation[3], but the nonaxial positioning of the implants makes clearance of important anatomical structures difficult to ascertain intraoperatively. Remote anchorage options such as zygomatic and pterygoid implants require great precision because important structures such as the orbital contents, maxillary artery, and the pterygoid venous plexus are distant to the initial instrumentation site (crestal level)[4–8], and are difficult to visualize within the operative field of view during instrumentation. When iatrogenic injuries do occur, it is often after the structure of interest has been violated that the clinician is able to recognize and react. Due to these important considerations, various surgical techniques including static and dynamic guides and surgical technical modifications have been developed[9–16] to aid the clinician in circumventing surgical pitfalls. The accuracy data of these techniques have been encouraging at the present time[10,11,17–20], but the evidence has not been as abundant or robust with respect to the analysis methods with which these techniques were analyzed.

Several methods have been used to analyze implant surgical accuracy, including manual measurement of implant position on computed tomography[21] (CT) and various superimposition techniques, with manual measurement[10] or manipulation[11]. Of the superimposition techniques, surface-based registration (SBR) involves overlaying surface meshes of the postsurgical implant on the planned virtual implant. The postsurgical implant mesh can be derived from segmentation of the CT volume[25], or a virtual implant manually overlaid onto the postsurgical CT implant[10,11,17]. However, all of these techniques suffer from CT metallic artifacts, which make precise comparison with the preoperative plan difficult. Whether direct manual measurements are made on the CT implant[21], or whether digital implant analogs are superimposed onto the CT implant[23,23,24,26], in lack of

[1]Department of Oral and Maxillofacial Surgery, University of Illinois Chicago College of Dentistry, 801 S. Paulina St., Room 110, Chicago IL 60612 – 7211, USA. [2]Private Practice Oral and Maxillofacial Surgeon, Chicago, IL, USA. [3]Department of Restorative Dentistry, University of Illinois Chicago College of Dentistry, Chicago, IL, USA. ✉email: hanmd@uic.edu

clarity of the CT implant results in potential inaccuracies in making measurements or superimposing digital implant analogs[24]. Furthermore, when angular accuracy is measured on CT or on CT-generated meshes, there is even greater challenge because aligning the reference frame to the implant's local frame is difficult to verify. Moreover, none of these techniques using CT or CT-derived imaging only have been validated for accuracy in the literature, to the best of our knowledge. The use of scan bodies[24,25] aims to overcome these limitations, as it allows replication of the implant position without relying on CT imaging of the actual implant. However, despite the theoretical advantages, validation of the accuracy of this technique itself has been vulnerable to methodological challenges[28], and data is lacking on scan body-assisted SBR (SB-SBR) especially for zygomatic implants (ZI). In other words, the systematic errors – reproducible errors from flaws or inaccuracies in measurement tools or processes[26] - inherent to SB-SBR must be thoroughly analyzed in order to confidently appraise data generated from this technique. The purpose of the present study was to measure the error and accuracy of SBR using scan bodies (SB-SBR) for conventional implant (CVI) and ZI accuracy analysis, using a combined additive manufacturing and digital approach to supplement the existing data for CVI, and add to the knowledge gap on ZI. The null hypothesis was that SB-SBR yields errors not significantly different from 1° angularly, and 1 mm linearly. The specific aims were to calculate the difference between the planned implant position and the position of the implant calculated by SB-SBR.

Results

Normality test

The mean AE and LE for both CVI and ZI followed a normal distribution (P-value 0.091 to 0.671, Shapiro-Wilk test), except the yaw and overall AE in CVI ($P=0.036$ and 0.008, Shaprio-Wilk test). The raw AE and LE (i.e. non-averaged) for both CVI and ZI in the physical ground truth model followed a normal distribution (P-value 0.111 to 0.964, Shapiro-Wilk test), except for axial pitch and yaw (P-0.031, 0.022, Shapiro-Wilk test). Because the vast majority of the variables in the physical ground truth model followed a normal distribution, parametric testing was used. The raw AE and LE for CVI and ZI in the model-free virtual SB-SBR did not follow a normal distribution ($P\leq0.004$, Shapiro-Wilk test), and therefore was subject to nonparametric testing. Non-parametric testing was used to compare the physical ground truth and model-free virtual SB-SBR methods (Table 2).

Angular error

The mean angular error was 0.48° for CVI (95% CI 0.35, 0.60) and 0.90° for ZI (95% CI 0.69, 1.10). Both were greater than 0° ($P<0.001$), although lower than the 1° accuracy threshold. The mean difference between the 2 implant types was 0.42° (95% CI 0.16,0.68, $P=0.003$), showing greater error when performing SBR for ZI. Details of the angular accuracy analysis can be found in Table 1.

Linear error

The mean linear error at the apex was 0.95 mm (95% CI 0.90, 1.00) and 1.63 mm (95% CI 1.29, 1.98) for CVI and ZI, respectively. The mean linear error at the platform was 0.96 mm (95% CI 0.89, 1.04) and 0.27 mm (95% CI 0.22, 0.33) for CVI and ZI, respectively. Both were significantly greater than 0 mm ($P<0.001$), with the linear apical error of the ZI exceeding the 1 mm accuracy threshold. The mean difference of linear error at the apex between the 2 implant types was 0.68 mm (95% CI 0.33, 1.03 $P=0.002$), showing greater error when performing SB-SBR for ZI. The mean difference at the platform, was 0.69 mm (95% CI 0.60, 0.79, $P<0.001$), showing greater error when performing SB-SBR for CVI.

A model-free, virtual SB-SBR showed overall angular errors of 0.84° and 0.38° for CVI and ZI, respectively (Table 2). The mean apical and platform linear errors were 0.81 and 0.86 for CVI, and 0.64 and 0.11 for ZI, respectively. With the exception of overall angular and pitch errors, the virtual SB-SBR showed lower errors than the anatomical model method.

Discussion

When designing or interpreting quantitative studies, the method of data acquisition warrants as much scrutiny as the data outputs. In other words, data interpretation must be accompanied by critical appraisal of the systematic errors associated the measurement technique. This is particularly important in implant dentistry,

Angular Error (°)	Conventional Implant Mean Absolute Error (95% CI)	Zygomatic Implant Mean Absolute Error (95% CI)	*P*-value†
Overall	0.48 (0.35, 0.60)	0.90 (0.69, 1.10)	0.003
Pitch	0.84 (0.74, 0.94)	0.67 (0.35, 0.99)	0.308
Roll	0.40 (0.20, 0.60)	1.25 (0.87, 1.63)	0.002
Yaw	0.20 (0.17, 0.22)	0.77 (0.39,1.15)	0.008
Linear Error (mm)			
Apex	0.95 (0.90, 1.00)	1.63 (1.29, 1.98)	0.002
Platform	0.96 (0.89, 1.04)	0.27 (0.22, 0.33)	< 0.001

Table 1. Angular and linear errors of surface-based registration technique for conventional and zygomatic implants. Abbreviations: CI – confidence interval. †Paired t-test.

	Anatomical Model			Virtual			Anatomical -Virtual			
	Conventional (mean, 95% CI)	Zygomatic (mean, 95% CI)	*P*-value*	Conventional (median, 95% CI)	Zygomatic (median, 95% CI)	*P*-value**	Conventional (median, 95% CI)	*P*-value**	Zygomatic (median, 95% CI)	*P*-value**
Angular										
Overall	0.57 (0.40, 0.73)	1.41 (1.02, 1.81)	< 0.001	0.20 (0.28, 0.51)	0.40 (0.30, 0.46)	0.975	0.10 (0.16, 0.41)	0.063	1.15 (0.87, 1.48)	< 0.01
Pitch	0.84 (0.64, 1.04)	1.03 (0.40, 1.66)	0.59	0.80 (0.80, 0.84)	0.40 (0.25, 0.37)	0.004	0.15 (0.13, 0.38)	0.858	0.65 (0.52, 1.30)	0.074
Roll	0.66 (0.28, 1.04)	2.04 (1.26, 2.82)	0.005	0.10 (0.10, 0.14)	0.55 (0.34, 0.55)	0.008	0.45 (0.30, 0.80)	0.015	1.50 (1.18, 2.14)	0.007
Yaw	0.20 (0.15, 0.25)	1.17 (0.45, 1.90)	0.013	0.20 (0.18, 0.20)	0.50 (0.24, 0.50)	0.025	0.05 (0.03, 0.07)	0.655	0.70 (0.59, 1.40)	0.058
Linear										
Apex	1.10 (0.99, 1.20)	2.62 (1.95, 3.29)	< 0.001	0.81 (0.76, 0.83)	0.84 (0.45, 0.78)	0.646	0.25 (0.18, 0.40)	0.007	2.15 (1.44, 2.48)	0.005
Platform	1.06 (0.92, 1.21)	0.43 (0.33, 0.53)	< 0.001	0.88 (0.85, 0.88)	0.15 (0.07, 0.14)	0.005	0.20 (0.14, 0.32)	0.022	0.33 (0.22, 0.42)	0.005

Table 2. Comparison of angular and linear absolute errors using anatomical model and virtual methods. Abbreviations: CI – confidence interval. Paired t-test* Wilcoxson signed- rank test**.

where accuracy is measured in fractions of a millimeter or degrees. The present study aimed to validate the angular and linear accuracy of SB-SBR, a technique with several theoretical advantages to direct measurement or manual manipulation techniques.

The findings of the present study are nuanced and warrant cautious and critical interpretation based on the clinical context in which SB-SBR is to be utilized. Regarding AE, SB-SBR showed acceptable levels of overall angular accuracy for both CVI and ZI (under the 1° threshold), however, when broken down into pitch, roll, and yaw errors, ZI had an angular error of 1.25° for roll. The reason AE was further analyzed into pitch, roll, and yaw was to determine whether there were high errors that would be masked if only the composite AE would have been calculated. In addition, pitch, roll, and yaw errors can offer insight into the directionality of errors which can be critical for dental implant placement, as the directionality of rotational errors correlate with the directionality of LE[30]. In a study analyzing the AE and LE in regional voxel-based registration, Han et al. showed that roll and yaw errors correlated with mediolateral errors, pitch and roll with vertical errors, and pitch and yaw with anteroposterior errors[27]. When extrapolating to the present study's findings, the higher angular error in roll can result in greater mediolateral and vertical linear errors at the apex of an implant. For a ZI, this could result in the apex of an accurately placed implant erroneously assessed as being in the orbit or infratemporal fossa. Regarding LE, the apical LE exceeded the 1 mm threshold in ZI, measuring 1.63 mm. As described in the Methods section, the 1 mm LE threshold was based on the clinical judgement of a reasonable safety margin at a remote anchorage site in ZI placement, where sufficient clearance must be planned to avoid violating the orbit and the infratemporal fossa, and to prevent failure of engaging sufficient bony anchorage. When applying a 1–2 mm safety margin used in other types of dental implants,[31] the 1.63 mm apical LE for ZI means that a ZI placed into the orbit can be erroneously assessed as safely clearing the orbit, or a well-placed ZI could be erroneously assessed as violating an important anatomic structure or not achieving sufficient osseous anchorage. When translating such observations to protocol development, the observed LE associated with SB-SBR could lead to overly lenient or stringent development of protocols if ZI accuracy data based on SB-SBR were to be relied upon. It was interesting to note that the linear error was lower at the platform for the ZI despite the opposite at the apex. This could be attributed to the broader surgical area in the posterior maxilla, and therefore a greater mutual region of interest for superimposition of the SM to the preoperative CT.

The focus and strengths of the present study were in the multi-faceted efforts to create an accurate ground truth against which SB-SBR attempts could be compared. Unlike other procedures such as orthognathic surgery, the structure of interest in dental implant surgery is metallic, and therefore prone to metallic artifacts on postoperative three-dimensional imaging. These artifacts create several challenges that could make direct comparison impossible. First, the artifacts obscure the precise boundaries and make it difficult to accurately make direct measurements or to superimpose surface meshes properly. In addition, segmentation of the CT implant results in a poorly defined surface mesh, making subsequent SBR with a virtual implant inaccurate. Investigating the accuracy of SB-SBR is complicated by the fact that a physical replica of the scan body-jaw complex is required, and that fabricating an error-free replica is neither feasible nor readily verifiable. While some methods such as micro-CT are used in fields such as endodontics[32], studies demonstrate artifacts in the presence of metallic objects[30,31]. In addition, errors can occur when micro-CT is used in large objects requiring a larger field of view (such as the maxillary model used)[34], similar to errors with optical scanning of large objects[32]. With full recognition of the element of error in the ground truth replica, the present study employed a multi-faceted approach to minimize errors related to ground truth fabrication. The first was use of stereolithographic printing, which has shown to be a more accurate 3D printing methods for dental use, compared to direct light processing[33,34]. Creating a solid model with an offset channel (Fig. 1) was intended to minimize deviation of the implant angulation during placement, as deviation would have likely resulted in visible breakage or distortion of the solid model. However, it must be acknowledged that verification of depth was limited to visual assessment of the platform and apex, necessitating additional measures to mitigate the limitations of the fidelity of the physical ground truth model. For this purpose, the authors incorporated a second, model-free virtual SB-SBR to analyze the influence of manufacturing artifacts of physical replicas. Because this virtual SB-SBR did not involve scanning of a physical scan body and surrounding anatomy as is the case in clinical practice, the measured errors using the virtual SB-SBR would be a gross underestimation of the true error of SB-SBR, and the true error of SB-SBR likely lies between those calculated from the two techniques used in this study. For this reason, the outcome

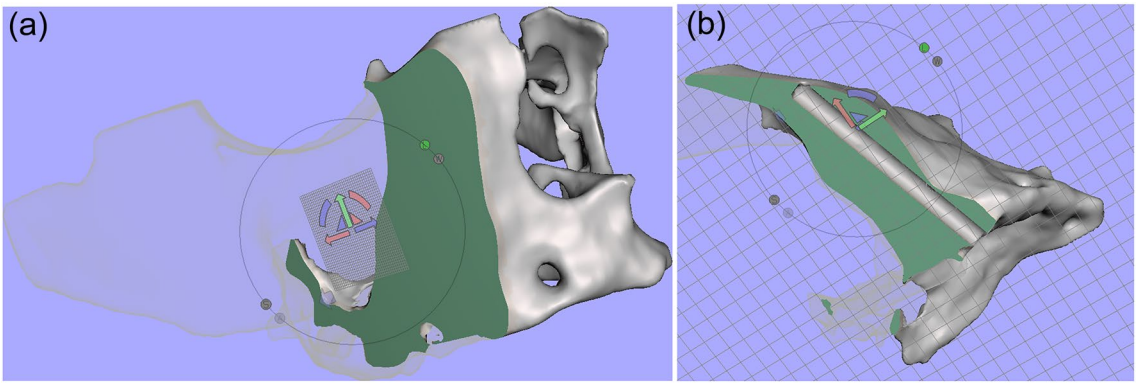

Fig. 1. The segmented midface was made completely solid, obliterating the maxillary sinus and the marrow space. This was to minimize deviation of the physical implant during placement into the 3D printed model. All images acquired from steps from Meshmixer version 3.5.474 (Autodesk, San Francisco, California https://www.autodesk.com/).

measure was obtained by calculating the mean of those measurements obtained from these 2 methods which served as upper and lower boundaries of errors.

In a meticulous in vitro accuracy validation study on SB-SBR[38], Oh and Lee created the ground truth model by exposing half of the physical implant threads through model trimming, followed by optical scanning and subsequent SBR using the remaining dentiform model as the mutual region of interest. Similar to the present study, this allowed a direct comparison of the planned and actual implant in surface mesh form, without relying on manual matching methods. However, the findings of our study differ significantly from those of Oh and Lee, which showed much lower angular (0.2°) and linear (0.05 to 0.08 mm) errors. The differences could be explained by the methodology, specifically the steps taken to create the ground truth model. Oh and Lee's protocol required 7 steps (1 physical grinding of model, 3 optical scans, 3 SBR), prior to SBR analysis of the actual and planned implants, whereas the present study required 6 (1 segmentation, 1 3D printing, 1 physical implant placement, 1 optical scanning, 2 SBR). It could be argued that fewer steps would yield smaller errors in ground truth design, and the mechanical subtractive methods used in Oh and Lee's study could potentially be prone to errors[35]. Specifically, Oh and Lee's study involved grinding of a dentiform model with a titanium implant placed to expose half of the implant surface, which was scanned and served as the mutual region of interest for superimposing a virtual implant analog. Grinding of interfacing structures present challenges, and require specialized techniques as is the case with histologic sectioning of biological tissue with metallic implants[35]. It is reasonable to suspect systematic errors from the grinding process, such as displacement or distortion of the implant, thus affecting the fidelity of the ground truth model. Also, this protocol required more optical scanning and SBR, one of which was the half-exposed implant surface, a small mutual region of interest which could elevate the risk of propagation of registration errors[36]. Despite the theoretical advantages and disadvantages, it is difficult if not impossible to compare the cumulative error of these steps, as the study protocols were different. For example, the errors from the present study's one of two chosen methods of setting the ground truth – placement of implants into digitally created implant osteotomies (Fig. 1) – and those of Oh and Lee could not be quantified and attempts to do so would face the same fundamental challenges of creating a high-fidelity ground truth model. The inability to conclusively determine the fidelity of the ground truth model, and therefore the accurate reproduction of the virtually planned implant is a limitation of the present study. Within the limitations, the cumulative errors that could have propagated from the protocol could be estimated through literature and manufacturer data: 0.13 mm for segmentation, up to 0.19 mm from SBR (not with SB); and for the 3D printed model, 0.1 mm for stereolithographic 3D printing, and up to 1.38 mm for implant placement[9]. However, as described, several measures were taken to mitigate this shortcoming[32,33] namely use of stereolithographic printing and employing a second model-free virtual SB-SBR, and calculating the estimated errors by averaging the upper (SB-SBR with physical ground truth model) and lower (model-free virtual SB-SBR) extremes. The authors believe establishing upper and lower boundaries of error could be more viable than incorporating a validation technique (e.g. micro-CT, optical scan), which could add variables that cannot be controlled for.

Another limitation of the present study was the lack of inter-examiner error measurement, as only one examiner obtained all scans. Furthermore, several software were used owing to the absence of a single (or fewer) software capable of performing all steps of the study, which could also influence external validity of the results. Lastly, the present study did account for scan body geometry, scanner and 3D printing specifications, warranting caution in extrapolating to different settings.

In conclusion, despite the theoretical advantages of SB-SBR given the lower reliance of manual manipulation and matching, the inherent errors may limit SB-SBR's usefulness when measuring linear errors for ZI, especially when used for tasks requiring high precision. Such cases may include surgical protocol development to lower surgical error margins of current techniques, and challenging cases with narrow margins of error (e.g. hypoplastic zygomas with the malar body close to the orbit). Existing data derived from SB-SBR must take into account the potential range of systematic errors inherent to the technique. Accuracy validation of SB-SBR using different

parameters is warranted, as well as accuracy validation of other methods such as direct measurement or manual manipulation to find a more accurate dental implant accuracy analysis tool.

Methods

Study design and ethical approval

The authors designed an in-vitro study using digitized and 3D-printed models of an atrophic edentulous maxilla. CVI and ZI were digitally planned and subsequently placed in a 3D-printed model. Using SB-SBR, the angulation of the physical dental implants was compared with those of the virtually planned implants. Ethical approval was exempted by the Institutional Review Board of the University of Illinois Chicago (Study ID 2024 – 1231).

The study protocol is detailed in the following subsections and is illustrated in Fig. 2.

Model design and implant placement

Full-field cone-beam computed tomography (CBCT) of an atrophic maxilla was segmented to create a stereolithographic (STL) surface using Dolphin 3D version 11.95 (Dolphin Imaging and Management Solutions, Chatsworth, California). Using freeform software (Meshmixer version 3.5.474, Autodesk, San Francisco, California), the mandible was removed and surface defects were repaired. This was imported back to Dolphin 3D, resulting in a midfacial STL surface accurately overlaid onto the CBCT volume. This composite skull was used to virtually plan an anterior CVI (4.0 × 10 mm) and a right ZI (4.0 × 45 mm), using a cylindrical analog of 4.1 × 10 mm and 4.1 × 45 mm, respectively.

Using Meshmixer, the cropped and repaired STL of the atrophic maxilla was made completely solid to obliterate the maxillary sinus as well as the marrow space (Fig. 1), and was split into the right midface and anterior maxilla.

The virtually planned implant analogs were digitally subtracted from the solid models. These models were 3D printed using a stereolithographic 3D printer (Form 3B+, Formlabs, Somerset, Massachusetts) using photopolymerized resin (Grey V4, Formlabs, Somerset, Massachusetts) and post-processed according to manufacture instructions. A 4.0 × 10 mm CVI (NeoDent GM Helix, Straumann Group, Basel, Switzerland) and a 4.0 × 45 mm ZI (4.0 × 45 mm, NeoDent Zygoma GM, Straumann Group, Basel, Switzerland) were placed into their respective offset slots by a single practitioner with significant experience with these systems (SG). The solidification of the models was to prevent deviation of the physical dental implants from the planned insertion

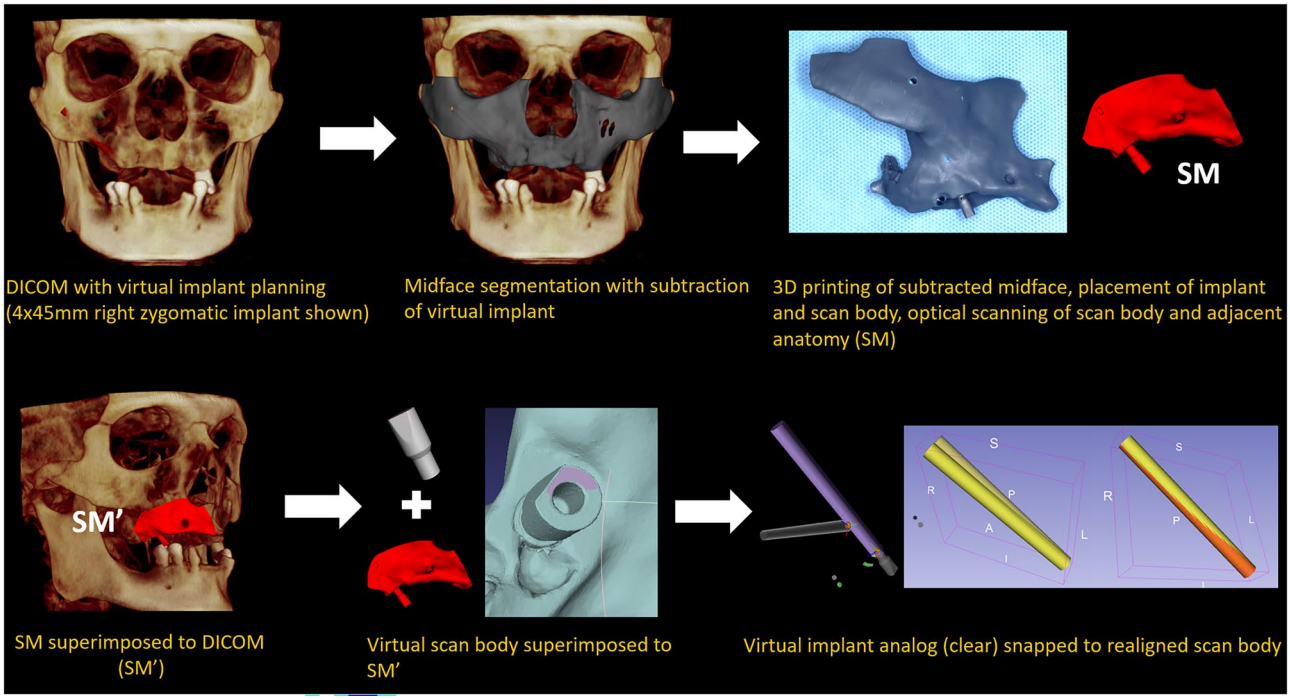

Fig. 2. Digital workflow from data acquisition to accuracy analysis. The implant was placed into a 3D printed maxilla with the virtually planned implant digitally subtracted. An optical scan was taken with the scan body attached, which was superimposed to the DICOM, creating a composite skull with the implant and scan body aligned to the coordinate system of the DICOM. A virtual scan body was superimposed to SM, to create SM'. A virtual implant analog was "snapped" onto SM', and its position was compared with the virtually planned implant using surface-based registration. The figure shows right zygomatic implant only. The same protocol was followed for the anterior conventional implant. Abbreviations: DICOM, Digital Imaging Communications in Medicine; SM, scan body-model scan. All images acquired from steps from Dolphin 3D version 11.95 (Dolphin Imaging and Management Solutions, Chatsworth, California), MeshLab version 2021.10 (Visual Computing Lab, Pisa, Italy), 3D Slicer (https://www.slicer.org/, version 5.1.0).

path, and the 0.1 mm offset was to prevent warpage or fracture of the model. The resultant experiment model was to represent as accurate of a reproduction of the virtual implants as possible.

Scanning protocol and virtual workflow

Following fabrication of the experiment model, the data acquisition process aimed to replicate the clinical steps of performing SB-SBR, and is further illustrated in Fig. 2 starting from the third step. The steps were as follows (Fig. 3):

1. A scan body (NeoDent GM, Straumann Group, Basel, Switzerland) was attached to the implants and the models with the scan bodies were scanned using an optical scanner (Trios 3, 3Shape, Copenhagen, Denmark).
2. The scan body-model scans (SM) were superimposed to the CBCT in Dolphin 3D, aligning the coordinate systems. A virtual version of the scan body obtained from the manufacturer's digital library was superimposed to the realigned SM (SM') via SBR using MeshLab version 2021.10 (Visual Computing Lab, Pisa, Italy), aligning the virtual scan body to the CBCT.
3. Using the "Create FaceGroup", "Create Pivot", and "Align" features of Meshmixer, the platform of the corresponding virtual implant analog was "snapped" onto the center of the platform of the virtual scan body, thereby replicating the position of the physical dental implant onto the coordinate space shared by the DICOM and all STL surfaces.
4. The virtually planned implant analog was superimposed to the snapped implant analog using SBR in 3D Slicer (version 5.1.0). The angular and linear changes were obtained from the transformation matrix, representing the difference between the virtually planned implants, and their physical replicas.

Ten separate SBR attempts were made for each implant type, based on sample size calculation with an alpha of 0.05, power of 0.80, and an effect size of 1.0, based on the chosen accuracy thresholds described in the description of the study variables. This yielded a sample size of 10 per implant type.

To account for inaccuracies of the 3D-printed experiment model, a virtual SB-SBR protocol was performed in conjunction. This involved superimposing a virtual scan body-alveolar bone complex to the DICOM, followed by SBR of a virtual scan body, and subsequent snapping of a virtual implant. This virtual SB-SBR did not involve optical scanning of the physical replica (i.e. 3D printed skull with physical implant and scan body, which could have errors inherent to the manufacturing process). Therefore, it did not have any artifacts attributable to the manufacturing process. However, because the virtual SB-SBR did not involve scanning of a physical object as is the case in clinical practice, it only partially represents errors inherent to SB-SBR, and therefore, the lower extreme of SB-SBR error.

Predictor and outcome variables

The primary predictor variable was the type of dental implant planned and placed (conventional, zygomatic). The primary outcome variable was the angular error, defined as the mean of the absolute value of the difference between the angle of the virtually planned and physically placed dental implants obtained from the 3D printed model-based SB-SBR and the virtual SB-SBR, respectively (°). The secondary outcome variable was linear error, defined as the mean of the 3D linear distance between the virtually planned and physically placed dental implants at the apex and the platform from the model-based and virtual SB-SBR protocols, respectively (scalar measurement in millimeters). Accuracy thresholds of 1° and 1 mm were set for angular and linear error, respectively. The rationale for these thresholds were based on the authors' clinical judgement of an acceptable safety margin at the most remote site (apex of a ZI). Given the proximity to important structures like the orbit, a registration-related error of 1 mm was deemed minimally acceptable, as the addition of surgical placement error

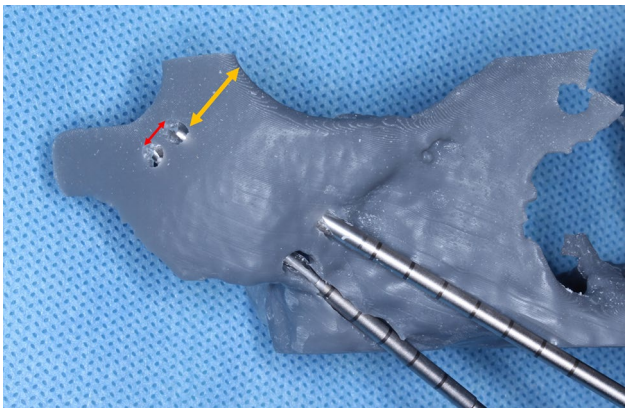

Fig. 3. The apical region of a zygomatic implant can be in close proximity to the orbit (gold double line), the infratemporal fossa (not shown), or the apex of another zygomatic implant (red double line). When a 1–2 mm safety clearance for surgery is applied as in conventional dental implants, a 1 mm threshold of linear error from scan-body-assisted surface-based registration was deemed clinically relevant for this investigation.

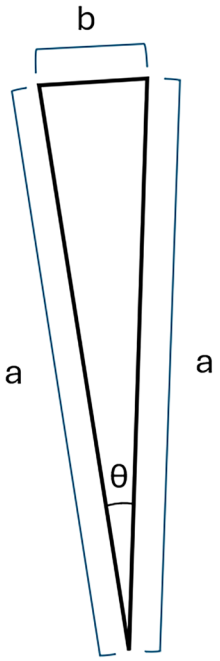

$$b = \sqrt{a^2 + a^2 - 2a^2\cos\theta}$$

θ	a	b
1°	10mm	0.17mm
1°	55mm	0.96mm

Fig. 4. The angular accuracy threshold of 1 degree (ϑ) was based on the calculated linear error at the implant apex (b). For a longer zygomatic implant of 55 mm, the linear error at the apex with a 1 degree angular deviation is 0.96 mm.

could lead to violation of such important anatomical structures. Using a long ZI length of 55 mm, an error of 1° led to an error of approximately 1 mm at the apex (Fig. 4).

Statistical analysis

Normality testing was performed using Shapiro-Wilk test. Paired t-test (for normally distributed variables) and Wilcoxon signed-ranked tests (for non-normally distributed variables) were used to compare the angular and linear errors for CVI and ZI. One-sample t-test and one-sample Wilcoxon signed- ranked test were used to compare the angular and linear errors to their established accuracy thresholds. The level of statistical significance was set at $P < 0.05$.

Statistical analysis was performed using SPSS version 28.0.1.1 (IBM Corporation, Armonk, New York).

Data availability

Data from this study is available upon request to the corresponding author.

Received: 27 April 2025; Accepted: 31 October 2025
Published online: 03 December 2025

References

1. Han, M. D. et al. What do we know beyond reliability in Voxel-Based registration? Validation of the accuracy of regional Voxel-Based registration (R-VBR) techniques for orthognathic surgery analysis. *J. Oral Maxillofac. Surg.* **80**, 296-302 (2022).
2. Rosenstein, J. & Dym, H. Zygomatic implants: A solution for the atrophic maxilla. Dental Clinics of North America vol. 64 Preprint at https://doi. (2020). https://doi.org/10.1016/j.cden.2019.12.005
3. Cooper, L. F., Thalji, G. & Al-Tarawneh, S. Are nongrafting solutions viable for dental implant treatment in limited bone volume? *Compendium Continuing Educ. Dentistry*. **41**, 368–796 (2020).
4. Tran, A. Q. et al. Zygomatic dental implant induced orbital fracture and inferior oblique trauma. *Orbit (London)* **38**, 236-239 (2019).
5. Kämmerer, P. W. et al. Evaluation of surgical techniques in survival rate and complications of zygomatic implants for the rehabilitation of the atrophic edentulous maxilla: a systematic review. *Int. J. Implant Dent.* **9**, 1–16 (2023).
6. Valeron, J. F. & Valeron, P. F. Long-term results in placement of screw-type implants in the pterygomaxillary-pyramidal region. **22**, 195–200 (2007).
7. Candel, E., Penarrocha, D. & Penarrocha, M. Rehabilitation of the atrophic posterior maxilla with pterygoid implants: A review. Journal of Oral Implantology vol. **38** 461–466 Preprint at (2012). https://doi.org/10.1563/AAID-JOI-D-10-00200
8. Gaur, V., Doshi, A. & Palka, L. Multiple pterygoid approach: A novel technique with single-piece implants. *Natl. J. Maxillofac. Surg.* **13**, S228-S236 (2022).
9. Tahmaseb, A., Wismeijer, D., Coucke, W. & Derksen, W. Computer technology applications in surgical implant dentistry: A systematic review. *Int. J. Oral Maxillofac. Implants*. **29**, 26–42 (2014).
10. Emery, R. W., Merritt, S. A., Lank, K. & Gibbs, J. D. Accuracy of dynamic navigation for dental implant placement-model-based evaluation. *J. Oral Implantology*. **42**, 399–405 (2016).
11. Block, M., Emery, R., Lank, K. & Ryan, J. Implant placement accuracy using dynamic navigation. *Int. J. Oral Maxillofac. Implants*. **32**, 92–99 (2017).

12. Fortin, T., Champleboux, G., Bianchi, S., Buatois, H. & Coudert, J. L. Precision of transfer of preoperative planning for oral implants based on cone-beam CT-scan images through a robotic drilling machine: an in vitro study. *Clin. Oral Implants Res.* **13**, 651–656 (2002).
13. Vercruyssen, M., Fortin, T., Widmann, G., Jacobs, R. & Quirynen, M. Different techniques of static/dynamic guided implant surgery: modalities and indications. *Periodontol 2000*. **66**, 214–227 (2014).
14. Chiarelli, T., Franchini, F., Lamma, A., Lamma, E. & Sansoni, T. From implant planning to surgical execution: an integrated approach for surgery in oral implantology. *Int. J. Med. Rob. Comput. Assist. Surg.* **8**, 57–66 (2012).
15. Chow, J., Wat, P., Hui, E., Lee, P. & Li, W. A new method to eliminate the risk of maxillary sinusitis with zygomatic implants. *Int. J. Oral Maxillofac. Implants*. **25**, 1233–1240 (2010).
16. Chow, K. F. Stepwise osteotomy protocol for zygomatic implant placement under navigation in patients with extra-sinus trajectory. *Int. J. Oral Maxillofac. Surg.* **52**, 1286–1289 (2023).
17. Kim, M. J. et al. Accuracy of digital surgical guides for dental implants. *Maxillofac. Plast. Reconstr. Surg.* **44**, 1–8 (2022).
18. Gourdache, I., Salomo-Coll, O., Hernandez-Alfaro, F. & Gargallo-Albiol, J. Dental implant positioning accuracy using a key or keyless static fully guided surgical system: A prospective systematic review and meta-analysis. *Int. J. Prosthodont.* 1–38. https://doi.org/10.11607/ijp.8212 (2023).
19. Wang, W., Yu, X., Wang, F. & Wu, Y. Clinical efficacy of computer-assisted zygomatic implant surgery: A systematic scoping review. *J. Prosthet. Dent.* **1-13** https://doi.org/10.1016/j.prosdent.2023.10.032 (2023).
20. Yang, J. & Li, H. Accuracy assessment of robot-assisted implant surgery in dentistry: A systematic review and meta-analysis. *J. Prosthet. Dent.* **1–15** https://doi.org/10.1016/j.prosdent.2023.12.003 (2024).
21. Hernández-Alfaro, F. et al. Three-Dimensional evaluation of the accuracy of zygomatic implant placement through an In-House fully guided approach. *Int. J. Oral Maxillofac. Implants*. **38**, 747–756 (2023).
22. Block, M. S., Emery, R. W., Cullum, D. R. & Sheikh, A. Implant placement is more accurate using dynamic navigation. *J. Oral Maxillofac. Surg.* **75**, 1377-1386 (2017).
23. Cao, Z. et al. Pilot study of a surgical robot system for zygomatic implant placement. *Med. Eng. Phys.* **75**, 72–78 (2020).
24. El Kholy, K., Janner, S. F. M., Schimmel, M. & Buser, D. The influence of guided sleeve height, drilling distance, and drilling key length on the accuracy of static Computer-Assisted implant surgery. *Clin. Implant Dent. Relat. Res.* **21**, 101–107 (2019).
25. Oh, S. M. & Lee, D. H. Validation of the accuracy of postoperative analysis methods for locating the actual position of implants: an in vitro study. *Appl. Sci. (Switzerland)*. **10**, 1–10 (2020).
26. Taylor, J. R. & Thompson, W. An introduction to error analysis: the study of uncertainties in physical measurements. *Phys. Today* **51**, 57-58 (1998).
27. Han, M. D., Kwon, T. G., Miloro, M. & Chakrabarty, S. What is the linear accuracy of regional Voxel-Based registration for orthognathic surgery landmarks? *J. Oral Maxillofac. Surg.* **81**, 546556 (2023).
28. Piermatti, J. & Oyole, P. The mandibular canal: A study to determine if cortical bone exists as a protective roof for the inferior alveolar nerve. *J. Oral Implantol* **49**, 584-589 (2023).
29. Kalantar Motamedi, M. R., Mortaheb, A., Zare Jahromi, M. & Gilbert, B. E. Micro-CT Evaluation of Four Root Canal Obturation Techniques. Scanning 6632822 (2021). (2021).
30. Liu, S., Broucek, J., Virdi, A. S. & Sumner, D. R. Limitations of using micro-computed tomography to predict bone-implant contact and mechanical fixation. *J. Microsc.* **245**, 34–42 (2012).
31. du Plessis, A., Broeckhoven, C., Guelpa, A. & le Roux, S. G. Laboratory x-ray micro-computed tomography: a user guideline for biological samples. *Gigascience* **6**, 1–11 (2017).
32. Ender, A. & Mehl, A. In-vitro evaluation of the accuracy of conventional and digital methods of obtaining full-arch dental impressions. *Quintessence Int.* **46**, 9–17 (2015).
33. Németh, A. et al. Clear guidance to select the most accurate technologies for 3D printing dental models – A network meta-analysis. Journal of Dentistry vol. 134 Preprint at (2023). https://doi.org/10.1016/j.jdent.2023.104532
34. Chen, Y., Li, H., Zhai, Z., Nakano, T. & Ishigaki, S. Impact of internal design on the accuracy of 3-dimensionally printed casts fabricated by stereolithography and digital light processing technology. *J. Prosthet. Dent.* **130**, 381.e1-381.e7 (2023).
35. Kunert-Keil, C., Richter, H., Zeidler-Rentzsch, I., Bleeker, I. & Gredes, T. Histological comparison between laser microtome sections and ground specimens of implant-containing tissues. *Annals Anat.* **222**, 153-157 (2019).
36. Shah, M., Franaszek, M. & Cheok, G. Propagation of error from registration parameters to transformed data. *J. Res. Natl. Inst. Stand. Technol.* **121**, 196-221 (2016).
37. Friedli, L., Kloukos, D., Kanavakis, G., Halazonetis, D. & Gkantidis, N. The effect of threshold level on bone segmentation of cranial base structures from CT and CBCT images. *Sci. Rep.* **10**, 7361 (2020).
38. Han, G. et al. A comparison of voxel- and surface-based cone-beam computed tomography mandibular superimposition in adult orthodontic patients. *J. Int. Med. Res.* **49**, 300060520982708 (2021).
39. Formlabs Form 3 Dimensional Accuracy Report.
40. Kim, S. Y. et al. Precision and trueness of dental models manufactured with different 3-dimensional printing techniques. *Am. J. Orthod. Dentofac. Orthop.* **153**, 144–153 (2018).

Author contributions

Michael Han: Conceptualization, data curation, formal analysis, investigation, methodology, project administration, supervision, validation, writing of original draft and review and editing.Sebastian Graca: Conceptualization, investigation, methodology, writing (review and editing).Dima Ghunaim: Methodology, investigation, writing (review and editing)Leila Ahmadian: Methodology, investigation, writing (review and editing).

Declarations

Competing interests

The authors declare no competing interests.

Additional information

Correspondence and requests for materials should be addressed to M.D.H.

Reprints and permissions information is available at www.nature.com/reprints.

Publisher's note Springer Nature remains neutral with regard to jurisdictional claims in published maps and institutional affiliations.